Preferred citation: M. Fuchs, E.M. Charry, G. Böhm, R. Resel, R. Schennach and K. Zojer. Where is the water? In *Advances in Pulp and Paper Research*, Cambridge 2022, Trans. of the XVIIth Fund. Res. Symp. Cambridge, 2022 (D. Coffin and W. Batchelor, eds), pp 495–510. FRC, Manchester, 2022. DOI: 10.15376/frc.2022.1.495.

WHERE IS THE WATER?

Maximilian Fuchs[1,2], Eduardo Machado Charry[1,2], Gregor Böhm[1,2], Roland Resel[1], Robert Schennach[1,2] and Karin Zojer[1,2]

[1]Institute of Solid State Physics, NAWI Graz, Graz University of Technology, Austria
[2]Christian Doppler Laboratory for Mass Transport through Paper, Graz University of Technology, Austria

ABSTRACT

The imbibition of paper with water is a complex interplay between the transport of liquid water in the fiber network and a swelling of the fibers. While the swelling can be directly associated with the incorporation of water into the fibers, little is known how swelling affects the pore space in paper and the subsequent transport of liquids therein. In this work, the propagation of a water drop supplied to a sheet of paper is monitored in-situ using X-ray microcomputed tomography. This method provides a 3D image sequence that traces the time-dependent progression of swelling and liquid transport over a period between fifteen and forty-five minutes after the application of water. The associated water vapor appears to profoundly swell the fibers even before the liquid water front arrives, i.e., the water invades paper both in its liquid and its vapor state. Incorporation of water into fibers leads to a marked increase in sheet thickness that originates from an increase in fiber volume and, interestingly, from an effective increase of the volume of the pores. Whether the latter change in pore volume has an adverse or boosting effect on liquid transport cannot be established from the data because liquid water does not reside in interfiber pores. Instead, liquid water is found in the lumen of the fibers.

1 INTRODUCTION

The prevalent liquid transport mechanisms need to be identified to predict and control the water uptake and spread in paper. Important candidate mechanisms are swelling and interfiber pore filling. Particularly interesting is to distinguish the role that fibers and available pore space play in each of these, possibly competing mechanisms.

Three-dimensional in-situ imaging of paper microstructures promises to reveal a clear local view on water propagation and fiber swelling. With the help of confocal laser scanning microscopy it was shown that fiber diameters increase in the presence of water, but reversibly approach the initial value after drying. [1] Further, water was shown to undergo a fingering motion to get from one interfiber pore to another, a motion that combines periods of slow wetting with events of rapid completion of pore-filling. [1] A similar discontinuous motion has also been found for spontaneous imbibition of non-swelling yarns monitored with time-resolved X-ray microcomputed tomography (μ-CT). [2] μ-CT is an alternative and promising imaging method for in-situ studies of paper. Previous studies established that, first, μ-CT-scans are suitable to quantify volume changes of paper fibers after swelling, [3] and second, that changes in the fiber and fiber network structure occur on time-scales accessible to in-situ μ-CT. [4]

In this work, we use a sequence of consecutive μ-CT scans to time-resolve the propagation of a droplet of water, applied to the end of a paper strip, through paper. We intend to clarify (i) how fast and to which extent the pore space changes due to swelling, (ii) whether the fingering motion in the interfiber pores can be observed on the monitored time scale, and (iii) which pores are involved in this motion.

2 MATERIAL, IN-SITU MICROSTRUCTURE ACQUISITION, AND STATISTICAL ANALYSIS

2.1 Material

We consider the microstructure of an unbleached paper that consists of never-dried, fresh fibers. Softwood fibers, mainly from pine, were predominantly extracted from regional wood in a Kraft process. This paper does not contain intentional fillers, did not pass any mechanical post treatment, and has a basis weight of 100 g/m^2, confirmed by a test in accordance to the standard DIN EN ISO 536 (Paper and board: Determination of grammage). The paper contains 0.8 kg of the sizing agent alkenyl succinic anhydride per ton paper. The sizing results in a hydrophobic surface with a contact angle of 122 ± 5 degrees for water. The contact angle was measured using a CAM 200 from KSV Instruments LTD.

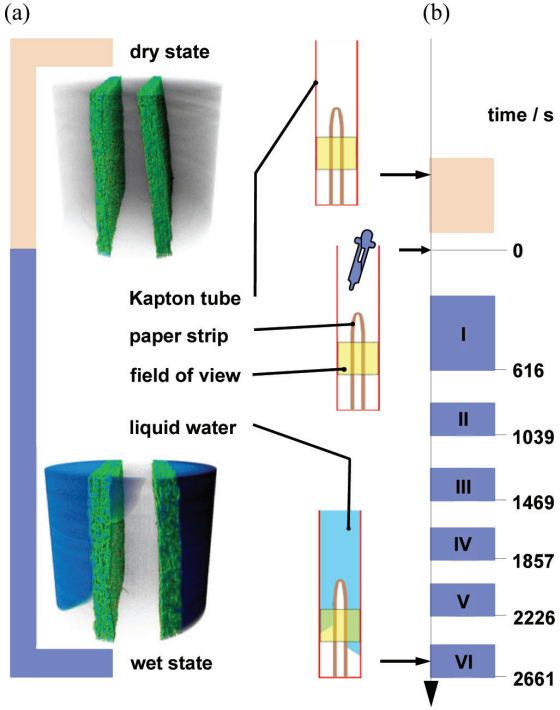

Figure 1. (a) Schematic drawing of the Kapton tube containing the paper sample before and after supplying a droplet. The scanned field of view is marked in yellow. Also shown are the associated rendered 3D images of the scanned volume before supplying the water (top) and after (bottom) completion of all scans after 2,661 s (ca. 45 min). The fibers are shown in green, water in blue, and air translucently. (b) Sequence and duration of scans I-VI to monitor the propagation of the water drop in the paper. A scan at ambient conditions (dry state) serves as reference.

Approximately 5μL droplets of purified water were applied to the specimens. The resulting static contact angles were evaluated via a Young-Laplace-Fit.

2.2 Microstructure Acquisition

As we need to anticipate changes in the pore and fiber geometries during the μ-CT scan, a sample layout must be used to prevent any additional, unintended motion of the scanned paper such as slipping or bending. Such a motion blurs the X-ray projections and lowers the resolution of the reconstructed image. However, it is desirable to avoid using any adhesive to fix the paper on the sample holder that can

potentially obstruct the free movement of the invading water. We account for these requirements by constructing the sample in the spirit of Neumann et al. [5] The scanned paper strip of the width 1.7 mm was folded once and inserted into a Kapton tube with an inner diameter of 1.8 mm (Figure 1a). The resulting tight fit prevents slipping or bending while permitting an unobstructed material expansion in the thickness direction and along the tube axis. In addition, care has been taken to align the long axis of the paper strip with the machine direction. A subvolume of the tube (highlighted in yellow in Figure 1a) was scanned at the TOMCAT beamline (Swiss Light Source at the Paul Scherrer Institute). This scanned volume corresponds to a field of view of 1.7 x 1.4 mm^2 with a final voxel size of 0.65 μm. A CMOS camera (pco.edge 5.5, 2,560 x 2,160 pixel) with a magnification of 10 was used. The imaging exploits absorption mode with an energy of 20 keV. In total, 1501 projections for the reference scan and 1001 for the wet scans were recorded over an angular range of 180 degrees with an exposure time of 250 ms. The tomographic reconstructions were performed by means of the Gridrec algorithm. [6]

Figure 1b describes the sequence of the performed scans. A scan of the paper sample in ambient conditions provided the reference microstructure to compare later changes to. In the following, we will refer to this reference sample as the dry sample. Then, the equivalent of one to two water droplets from a Pasteur pipette ($<0.1mL$) was supplied to the upper, open end of the tube. The central fold of the paper strip was located below this opening and several millimeters above the scanned volume (Figure 1a).

The supplied water droplet was not instantaneously sucked into the paper, but rather had to be gently forced into the tube. From the moment in which the water got visibly incorporated into the paper, six consecutive scans (I–VI) were acquired at regular offsets in time; the time stamp of each scan (noted in Figure 1b) refers to the time at which each scan was completed. Latest in scan II after 1039 s, liquid water that filled the gap between the tube and the exterior paper surface had arrived at the scanned volume. Hence, in all scans related to the wet state at least a portion of the scanned paper directly bordered liquid water.

2.3 Segmentation of 3D Images

A quantitative assessment of the location of liquid water and water-induced changes in the microstructure requires a segmentation of the raw 3D images of scans I-VI in terms of fibers, water, and air. Due to the inherently low absorption contrast and weak phase-contrast contribution at water-fiber interfaces (Figure 2c), we used a deep learning method for segmentation as provided by ORS Dragonfly. [7]. Convolutional neural networks (NN) have been trained to reliably distinguish the aforementioned constituents based on characteristic patterns. Such patterns include fiber and pore shapes and water-fiber interfaces with characteristic shapes

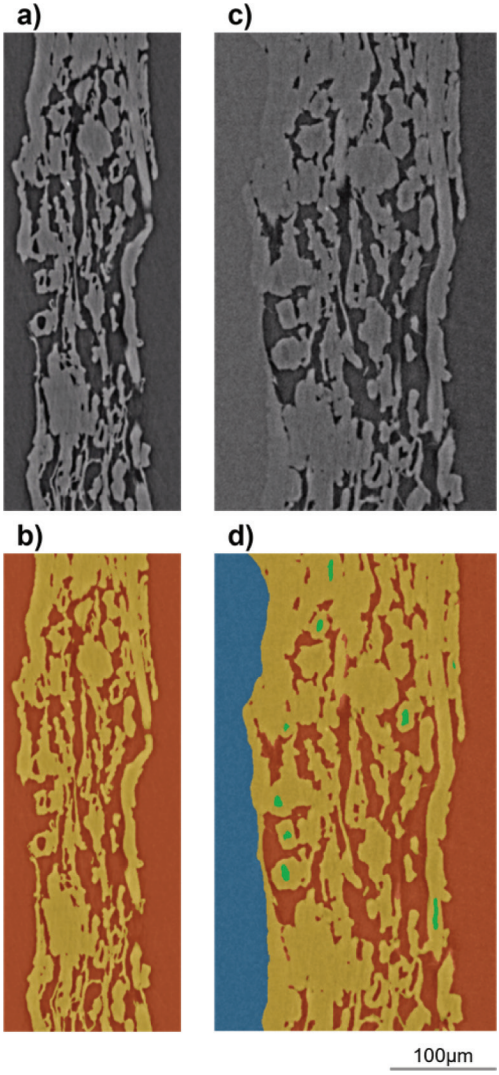

Figure 2. Excerpts of gray-scaled reconstructed μ-CT images from the dry state (a) and scan VI recorded 2,661 s after the application of the droplet (c). Related segmented images of the dry scan (b) and scan VI (d) showing dry and wet fibers (yellow), air (red), liquid water outside paper (blue), and liquid water inside lumen (green).

oriented in all three spatial dimensions. For a reliable identification of these patterns we used a pseudo 3D UNet architecture, [8, 9] because this neural network architecture is capable of recognizing a threedimensional context from 2D image stacks without the computational burden of using neural networks operating exclusively with 3D input image data. [9] To enhance the segmentation accuracy, two NNs were independently trained to provide two segmented data sets per raw image. While the first NN discriminates between air, fibers, and liquid water outside the paper sheet, the second NN finds voxels associated with enclosed liquid. For the sake of consistency, the dry scan was segmented with a third NN trained to distinguish between air and fibers. The quality of segmentation has been assessed with different metrics commonly used for NN-based segmentations. The related values and their interpretation are provided in the Appendix.

2.4 Statistical Analysis

Based on the segmented images, the volume occupied by fibers (dry and wet), by the pores between the fibers, and by the liquid water were determined. In the case of fibers and lumen, the volumina are directly given by the number of associated voxels times the voxel volume. Possible uncertainties of these values relate to the accuracy of voxel counting and arise from two factors. A first contribution arises from possibly misclassified voxels (e.g., fiber rather than air). Secondly, we may account for voxels that move out or in to the scanned field of view from one scan to another. Both uncertainties combined are expected to not exceed relative errors of 2.5% (cf. metrics of segmentation in the Appendix). To estimate the volume associated to the interfiber-pores, we first classified all air voxels into exterior voxels and internal air voxels between the fibers. While the former are located between the strips and between the strips and the tube, the latter are located in between the fibers and serve as estimate for the intrafiber pore space. A rolling ball algorithm with a ball radius of 35 μm implemented in the FIJI package [10] was applied to define an exterior paper surface that separates exterior and internal air voxels. [11] This radius of the ball probing the surface is expected to preserve all trends due to changes of the internal air volume, eventhough the computed volume depends on the somewhat ambiguous choice of the radius of the ball probing the surface. [12]

3 RESULTS

3.1 Motion of the Scanned Sample

The applied droplet moved along the tube from the top opening of the tube towards the bottom. On its way down, the droplet was split by the paper strips into two

portions. As shown in the schematic illustration in Figure 1, each of these water portions continued to move between the tube wall and the exterior surfaces of the folded paper strip. However, the water on the left side moved less fast than the water on the right hand side. By chance, the scanned field of view captured an intriguing asymmetric situation. The exterior surface of the right paper strip, i.e., the surface facing the tube, is in complete contact with water, while the exterior surface of the left paper is still partially exposed to air. The water did not penetrate the paper sheet so that that space in between the two paper strips is filled with air.

The paper strips considerably swell upon applying the water droplet. In line with previous experiments, [4] the swelling-induced changes in the thickness are almost completed within the first 10 min in scan I (not shown). Figure 1 suggests that the two strips visible in the scans moved slightly in sheet thickness direction. For a better comparison between the dry scan and scan VI, we additionally provide an overlay of cross-sections along the tube axis in the Appendix.

3.2 Location of Water

The cross-section shown in Figure 3 exemplifies the main observations related to the location of water in the paper. This cross-section belongs to the left strip. It is located in the lower region of the scanned volume (marked by an arrow in Figure 3a) and does not directly border liquid water. A visual inspection of the fibers in scans III and VI confirms that the fibers in the paper strip markedly swell upon exposure to the water droplet (shape A in Figure 3b). None of the pores visible in the reference scan (dry scan) appear to shrink but rather tend to increase in volume (scan III). More than 40 min have passed until the first detectable traces of liquid water (shape B in scan VI) arrive, i.e., 30 min after the paper completed most of the thickness change. That implies that fibers are considerably swollen before the liquid front arrives. This observation is consistent with the expectation that sizing hampers the liquid uptake via the pores [13] so that water is mainly taken up via sorption into the fibers. [14] In the shown cross-section, liquid water is exclusively found in a lumen of an almost uncollapsed fiber. In general, we find liquid water exclusively in the lumen across the sample. Even though we intensively searched for liquid water in the interfiber pores, neither inspection of the segmented images nor the visual screening of the reconstructed grey-scale images showed liquid water between fibers.

3.3 Effects of Water Propagation

The scan series allows us to quantitatively monitor how the liquid water penetrates into paper. As we do not find any liquid water in the interfiber pores, the propagation of water is going to affect these pores only indirectly.

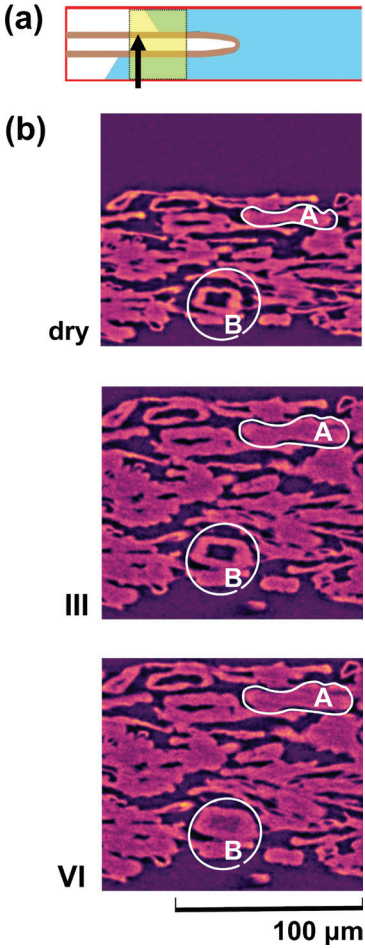

Figure 3. (a) Location of the two dimensional cross-section of a paper strip that is monitored as a function of time. (b) Evolution of the microstructure in this cross-section image in the dry state, 1,469 s (III) and 2,661 s (VI) after the application of the droplet. Shape A corresponds to a swelling fiber segment, while shape B marks non-collapsed lumen that is eventually filled with liquid water.

A large share of the initially offered water droplet is sorbed into the fibers. From the fiber fraction seen in our microstructure, we can directly determine how the volume related to fibers increases with time. Figure 4a shows the total volume of the fiber fraction in the field of view (blue dots) evolving with time. The fibers continuously swell and their volume steadily increases regardless which paper

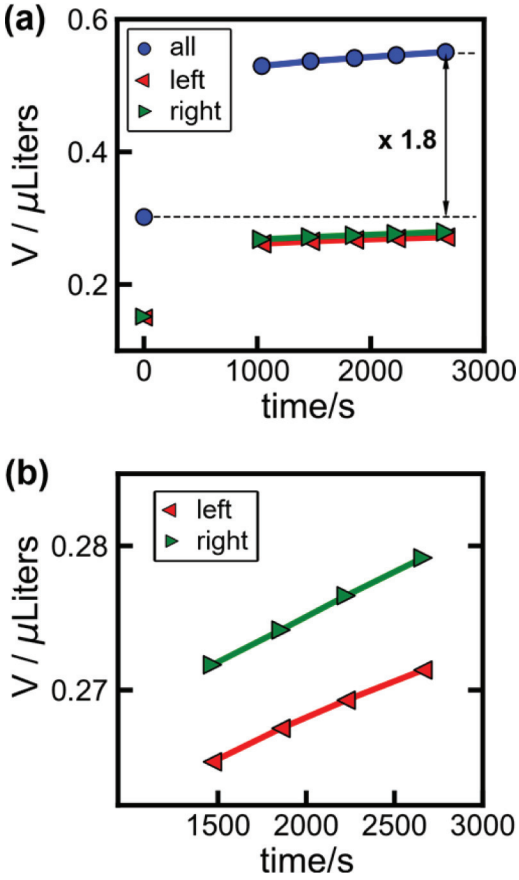

Figure 4. (a) Total fiber volume as a function of time (circles) and fiber volume associated with the left (red) and the right paper strip (green), respectively. The time is given with respect to the moment of applying the droplet to dry paper. (b) Closeup on the evolution of the fiber volume in the left (red) and right paper strip (green).

strip is considered (red and green symbols in Figure 4a). After completion of the final scan, the fiber volume does not tend to saturate, i.e., the swelling is still incomplete. On the contrary, the fibers in both strips increase their volume at a comparable, almost constant rate (Figure 4b). Such an ongoing expansion is to be expected considering the broad knowledge base related to moisture uptake of paper (e.g., [15, 16, 17]). In a particularly closely related experiment, a similar paper type exhibited a linear increase in paper mass and positron lifetimes in the same time range after humidity exposure. [18] Such positron lifetimes are obtained

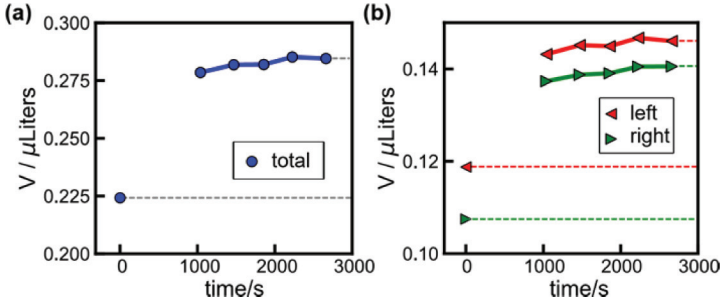

Figure 5. Evolution of the volume of pores with time. The time is given with respect to the moment of applying the droplet to dry paper. (a) Total volume *V* of pores in the sample, (b) pore volume *V* in the left (red) and right strip (green). The dashed lines serve as a guide to the eye to mark the total increase with respect to the dry state.

in positron-electron annihilation experiments and inform on changes in the pore space and in the chemical environment experienced by positrons.

The profound change in fiber volume readily suggests an impact on the pore space. To get an insight into the concomitant evolution of the pore space volume, we determined the volume of air-filled pores in the paper strips (Figure 5). Note that such pore volume only provide trends, because the values of the pore space volume depend on some ambiguity related to the definition of the paper surfaces (cf. Section 2.4). Regardless which paper strip is considered, the overall volume of the pores tends to increase by factor of 1.3 compared to the dry state (Figure 5b), as seen already at selected spots in the sample (cf. Figure 3). Also the volume change between consecutive scans does not show marked differences between the strips (Figure 5b). After 45 min, the expansion of the pore space volume is practically completed. The overall expansion implies that a large share of pores enlarge their volume during water uptake, in particular the ones that contribute most to the overall pore volume. This change in volume is accommodated by an overall increase in the sheet volume, that mainly translates into a sheet thickness increase.

The liquid water explores the paper exclusively in the lumen. At the time of scan II after 25 min we can identify lumen that are either filled completely already or partially filled. In the case of partially filled lumen, water progressively replaces air with time, but does not necessarily propagate from top to bottom. Rather, liquid "plugs" form in the lumen. These plugs appear regardless of the lumen orientation and without preference for the top parts of the lumen. Such plugs are illustrated in Figure 6 for two examples. Figure 6a) shows water in a ca. 1.4 mm long lumen segment. The color-coded regions represent the water content in this lumen after scan II (1,039 s, yellow), scan IV (1,857 s, red), and after the final scan VI (2,651 s, blue). The two air-filled regions that are enclosed by water plugs

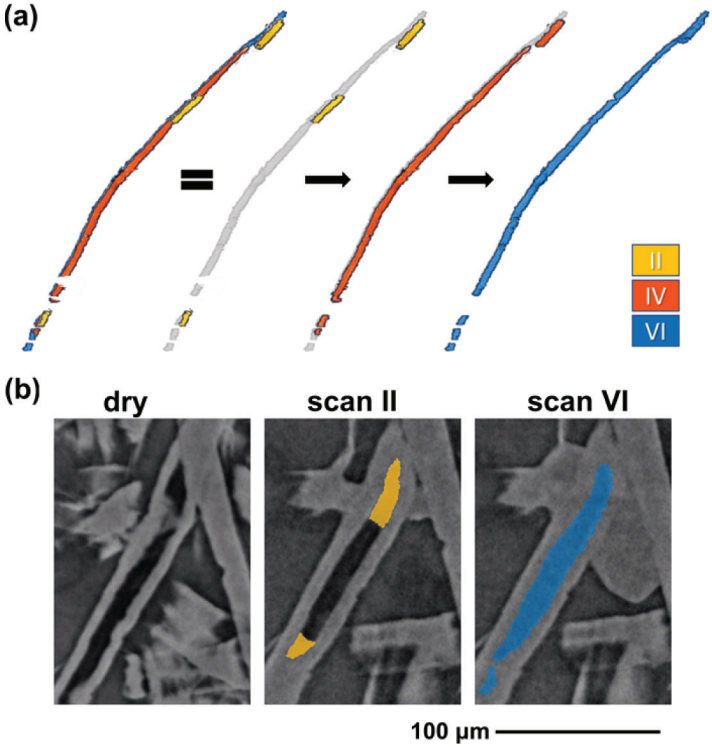

Figure 6. (a) The propagation of water is schematically shown for a selected lumen. From left to right, the filled portion found in scan II (yellow), scan IV (red), and scan VI (blue) is indicated. After scan VI, the entire lumen section contained in the field of view is filled. As a guide to the eye, the region associated with this entire section is shaded in gray. (b) Closeup on air displacement in a lumen. An empty lumen (dry) is partially filled with water (scan II) such that air becomes enclosed by two water plugs (yellow). The enclosed air bubble is completely replaced with water after scan VI.

in scan II (yellow) are completely filled with water after scan IV (red). A similar situation is shown in a closeup in Figure 6b). Here, a lumen segment initially filled with air (dry) is first closed off by two terminal plugs (blue in scan II) and, eventually, entirely filled with water.

The locally observed motion of water is in line with the associated increase in the observed volume of water (Figure 7). Figure 7a shows that the volume related to the total amount of liquid water as a function of time (blue) keeps increasing with time. However, the left and the right strip contribute differently to this increase (Fig. 7b) While the water stops propagating in the right strip after scan

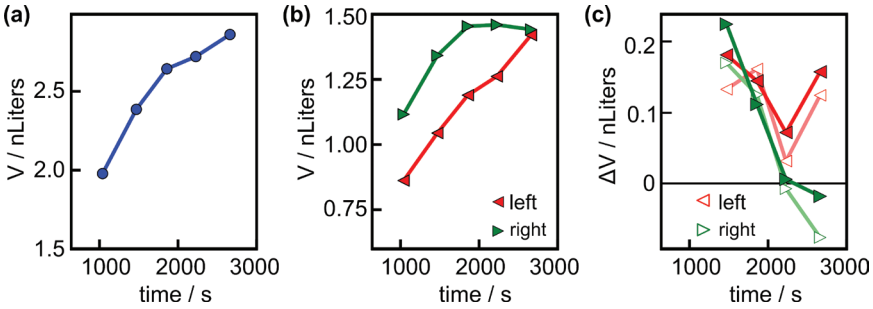

Figure 7. Evolution of the liquid water volume in the lumen with time. (a) The volume of the water-filled lumen in the entire sample (circle) and, (b), in the left (red triangles) and right strip (green triangles), respectively. (c) Change in volume, ΔV, as a function of time in the left (red triangles) and right strip (green triangles). Curves with open symbols represent strip-related volumes without considering clusters containing less than 2,000 voxels.

IV, there is still an ongoing increase in the left strip albeit at a reduced rate. Picturing the water transport as a successive filling of the lumen is further supported by the fact that most of the transported water moves in larger clusters. As shown in Figure 7c), the change in total water volume, ΔV, in each strip (filled symbols) is fully accounted for by the volume change of all water clusters exceeding 2,000 voxels in size (open symbols).

4 DISCUSSION

What remains puzzling is why liquid water is exclusively found in the lumen and how it entered the lumen. These questions cannot be unambiguously answered with the exploratory measurement shown here. However, our data suggests some critical remarks and also some likely explanations.

A possible initial filling of interfiber pores cannot entirely be ruled out, because our analysis starts only after 25 min after applying the droplet. In principle, this period of 25 min appears to be sufficient to allow liquid water to penetrate the interfiber pores in the scanned field of view. [19] Our inability to find any filled interfiber pores can only be explained by one of the following scenarios: First, liquid water might form a very thin film on the fiber walls. Such a thin film cannot be resolved in μ-CT, in particular, when no contrast agent is used. Given that our paper is hydrophobic such an efficient formation of thin films is not likely. A more plausible scenario is that water having been initially stored in the pores was

transported somewhere else. Most likely, the liquid water was quickly sorbed into the fiber walls. Our data on thickness and fiber volume expansion suggests that the water uptake is very efficient even though the paper is hydrophobic. It is unlikely that the water evaporated from the inner pore space while there is liquid water still covering the exterior surfaces.

As far as the filling of the lumen is concerned, also several mechanisms are conceivable: (i) Liquid water could enter lumen at the fiber ends, where the lumen are exposed to the interfiber pores, (ii) liquid water may enter from the interfiber pores via fiber pits, and (iii) water expelled from water-saturated fibers condenses in the lumen. The most important hint is that isolated droplets ("plugs") form in the lumen that do not move but rather increase in volume and eventually coalesce. Unless all of these plugs are exclusively seeded at the pits, a condensation of water supplied by the soaked fiber walls appears to be the most plausible explanation. A possible route to narrow down potential mechanisms of lumen filling is to clarify how the air that originally resided in the lumen is displaced. Such investigations call for a much stricter control of the humidity inside the sample compartment.

5 CONCLUSION

We demonstrate a highly promising approach to in-situ monitor the propagation of water in paper with a μ-CT-based approach. Future work has to assess whether this approach is sufficiently versatile to also look into other paper types, in particular into denser or unsized papers. Further optimization may permit an even better time resolution while keeping a submicrometer resolution. Our exploratory experiment readily highlights that the lumen may play a hitherto underestimated role in the transport of water in paper. The unexpected absence of liquid water in the interfiber pores can only be confirmed for the scanned volume. A statistically complete measurement probing several spots on the sheet is therefore called for. Nevertheless, temporary storage in the fibers and transport along the lumen appear to displace water in paper so efficiently, that the relative role of liquid propagation in the interfiber pores for observations times between a few seconds and several minutes should be reassessed.

ACKNOWLEDGMENT

The authors gratefully acknowledge financial support from the Christian Doppler Research Association, Federal Ministry for Digital and Economic Affairs, and the National Foundation for Research, Technology, and Development, Austria.

REFERENCES

[1] H. Aslannejad and S. M. Hassanizadeh. Study of Hydraulic Properties of Uncoated Paper: Image Analysis and Pore-Scale Modeling. *Transp. Porous. Med.*, 120:67–81, 2017.

[2] R. Fischer, C. M. Schlepütz, D. Hegemann, R. M. Rossi, D. Derome, and J. Carmeliet. Four-dimensional imaging and free-energy analysis of sudden porefilling events in wicking of yarns. *Phys. Rev. E*, 103:053101, 2021.

[3] R. Holmstad, A. Goel, S. Ramaswamy, and O. W. Gregersen. Visualization and Characterization of High Resolution 3d Images of Paper Samples. *Appita Journal: Journal of the Technical Association of the Australian and New Zealand Pulp and Paper Industry*, 59:370, 2006.

[4] J. F. Bloch and S. Rolland du Roscoat. Three-dimensional structural analysis. In Advances in Pulp and Paper Research, (ed. S. J. I'Anson), *14th Fund. Res. Symp.*, pp 599–664, Oxford, 2009.

[5] M. Neumann, E. Charry Machado, E. Baikova, A. Hilger, U. Hirn, R. Schennach, I. Manke, V. Schmidt, and K. Zojer. Capturing Centimeter-Scale Local Variations in Paper Pore Space via micro-CT: A Benchmark Study Using Calendered Paper. *Microscopy and Microanalysis*, 27:1–11.

[6] F. Marone and M. Stampanoni. Regridding reconstruction algorithm for real-time tomographic imaging. *J. Synchrotron Rad.*, 19:1029–1037, 2012.

[7] Dragonfly 2020.1, Object Research Systems (ORS) Inc, Montreal, Canada, 2020.

[8] O. Ronneberger, P. Fischer, and T. Brox. U-net: Convolutional Networks for Biomedical Image Segmentation. In Nassir Navab, Joachim Hornegger, William M. Wells, and Alejandro F. Frangi, editors, *Medical Image Computing and ComputerAssisted Intervention – MICCAI 2015*, Lecture Notes in Computer Science, pp234– 241, Cham, 2015. Springer International Publishing.

[9] M. H. Vu, G. Grimbergen, T. Nyholm, and T. Löfstedt. Evaluation of multislice inputs to convolutional neural networks for medical image segmentation. *Medical Physics*, 47:6216–6231, 2020.

[10] J. Schindelin, I. Arganda-Carreras, E. Frise, V. Kaynig, M. Longair, T. Pietzsch, S. Preibisch, C. Rueden, S. Saalfeld, B. Schmid, J.-Y. Tinevez, D. W. White, V. Hartenstein, K. Eliceiri, P. Tomancak, and A. Cardona. Fiji: An open-source platform for biological-image analysis. *Nature Methods*, 9:676, 2012.

[11] S. R. Sternberg. Biomedical image processing. *Computer*, 16:22–34, 1983.

[12] E. Machado Charry, M. Neumann, J. Lahti, R. Schennach, V. Schmidt, and K. Zojer. Pore space extraction and characterization of sack paper using micro-CT. *Journal of Microscopy*, 272:35–46, 2018.

[13] P. J. Salminen Water transport into paper- the effect of some liquid and paper variables. *Tappi J.* 195–200, 1988.

[14] J. S. Aspler. Interactions of ink and water with the paper surface in printing: A review. *Nordic Pulp & Paper Research Journal*, 8:68–74a, 1993.

[15] J. A. Bristow. Swelling of paper during sorption of aqueous liquids. *Svensk papperstidning*, 74:645–652.

[16] K. Niskanen, S. J. Kuskowski, and C. Bronkhorst. Dynamic hygroexpansion of paperboards. *Nordic Pulp and Paper Research Journal*, 12:103–110, 1997.
[17] A. Bandyopadhyay, H. Radhakrishnan, B. V. Ramarao, and S. G. Chatterjee. Moisture Sorption Response of Paper Subjected to Ramp Humidity Changes: Modeling and Experiments. *Ind. Eng. Chem. Res.*, 39:219–226, 2000.
[18] L. Resch, A. Karner, W. Sprengel, R. Würschum, and R. Schennach. Water intake of cellulose materials monitored by positron annihilation lifetime spectroscopy. *Cellulose*, 2021. DOI: 10.1007/s10570-021-04367-8 (early view)
[19] C. Waldner and U. Hirn. Ultrasonic Liquid Penetration Measurement in Thin Sheets—Physical Mechanisms and Interpretation. *Materials*, 13:2754, 2020.
[20] A. A. Taha and A. Hanbury. Metrics for evaluating 3D medical image segmentation: analysis, selection, and tool. *BMC Medical Imaging*, 15:29, 2015.

APPENDIX

A.1 Quality of Segmentation

For the segmentation of the μ-CT scans, convolutional neural networks were employed. Each of the three pseudo-3D UNet was trained on manually segmented images as ground truth. The quality of the segmented images predicted with the neural networks was assessed with the following commonly used metrics: The Dice coefficient and the Jaccard coefficient according to Taha et al. [20] and the categorical accuracy (CA) as the ratio between the number of correct predictions and the total number of predictions. Table 1 collect these coefficients for all scans. The accuracy, i.e., the percentage of predictions being correct, alone is not sufficient to judge the success of segmentation, in particular if the phase to be identified contains only a few voxels. Hence, the Jaccard index (intersection-of-union) was determined. In our case, the Jaccard index provides the ratio between the volume in which the prediction of the network matches the ground truth and the volume of the union between the predicted segmentation and the ground truth. The closer this index approaches unity, the better the prediction coincides with the ground truth (i.e., manually segmented images). The Dice coefficient is positively correlated to the Jaccard coefficient and, hence, reveals the same trends.

The segmentation of the wet scans using NN1 is inferior to the segmentation of the dry state with NNd. However, the regions misclassified by NN1 are located at the tube walls bordering water rather than being part of the paper strips. The segmentation of wet scans using NN2 to identify liquid water in the pores is less accurate than NN1 predictions, because the scanned volumes turned out to contain only a few voxels that can be classified as liquid water inside the paper sheet.

Table 1. Evaluation of the segmentation with the pseudo 3D UNet-type convolutional neural networks in terms of the Dice coefficient, the Jaccard coefficient and the categorical accuracy. Network NNd discriminates between fibers and air for the dry scan. Network NN1 discriminates between wet fibers, liquid water (excluding lumen), and air for scans II-VI. NN2 identifies liquid water enclosed by fiber.

NN	*Scan*	*Dice*	*Jaccard*	*Accuracy*
NNd	dry	0.9961	0.9924	0.9989
NN1	II	0.9779	0.9575	0.9778
NN1	III	0.9781	0.9576	0.9776
NN1	IV	0.9775	0.9568	0.9768
NN1	V	0.9759	0.9536	0.9755
NN1	VI	0.9781	0.9579	0.9779
NN2	II	0.8967	0.8537	0.9998
NN2	III	0.9131	0.8695	0.9998
NN2	IV	0.8916	0.8426	0.9998
NN2	V	0.8895	0.8423	0.9997
NN2	VI	0.9011	0.8491	0.9998

A.2 Motion of the Sample

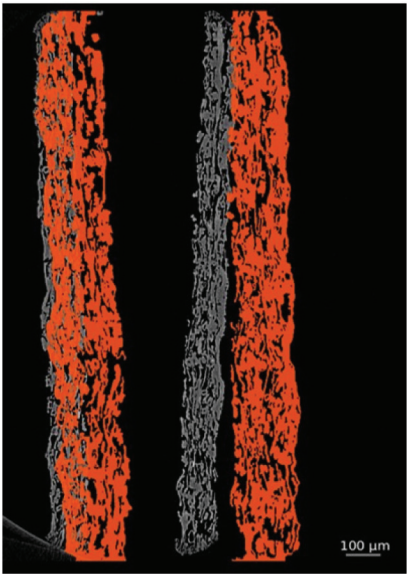

Figure 8. Overlay of a cross-section in the dry state (gray scale) and in the wet state, scan VI (orange). Upon adding the water droplet, the paper strips swell (thickness increase) and slightly move laterally.

WHERE IS THE WATER?

Maximilian Fuchs[1,2], *Eduardo Machado Charry*[1,2], *Gregor Böhm*[1,2], *Roland Resel*[1], *Robert Schennach*[1,2] *and Karin Zojer*[1,2]

[1] Institute of Solid State Physics, NAWI Graz, Graz University of Technology, Austria
[2] Christian Doppler Laboratory for Mass Transport through Paper, Graz University of Technology, Austria

Gil Garnier Monash University

I would like you to better define the objective and I explain. You show us a system with the contact angle of 122 degrees and said that it's thick, so my question is this: you have probably a line of border that has been digitised, so if this is the case what you will have is hydrophobic fibres and you will have absolutely no capillary flow within the paper. So that means at first the only way by which the water would go inside is they will have to diffuse to the cell wall, to the circular lumen, so that means there is no sizing, then the contacting surface is only the cell wall, you will have the capillary flow. So, are you trying to measure the diffusion constant of the water to the cell wall? What is your objective, that is the first question, and do you have the same work without any sizing to really understand the stick and slip mechanism?

Karin Zojer

So, we understand our work is just to see whether this technique is suitable or relevant for this process. So, we will not able to compete with scanning confocal laser microscopy. However, what we can do is we can first explore simple means to do the quantification. What we also can do is, or what possibly users could do, also use the measurements for other determinations as well. And one of the major things that has to be done and clarified in the near future is to properly define the

system to start with and to properly define the initial boundary conditions you are offering to the experiment, so what we have shown was by no means ideal. I have to say it was a test that worked on the spot, so the more you start to scrutinise what is going on, the more complicated it gets, of course. There are some commercial setups out there; however, they are not so well suited for our purpose, as the spatial resolution, at least at the the lab scale, is by no means as good. So, I think what you have mentioned is more or less a recipe how to go on. So, we have now a hydrophobised paper and we expect that of course the surface is getting most of the hydrophobisation effect. It would be better to have, I have to say, possibly a model paper where the hydrophobisation possibly had happened on the fibre level. What might be also enlightening to know is, even though I do not how to do this in a clever way, is to see what the hydrophobisation profile looks like in the first place. And the best specimen that I would hope for is a non-hydrophobised paper; however, this is going to challenge our ability to resolve everything in time. The transport is too quick for the time being. I am not a synchrotron expert but these guys are very, very active, so possibly in a few years from now this will become an option.

Gil Garnier

I understand, but I am very uncomfortable when you choose highly non-wetting conditions, so the enriching that you have is diffusion to the cell wall. Could it be an idea to reduce the sizing so the water contact angle is under 90 degrees, let's say 80 degrees, such as you will have some wetting, because now you completely precluded any flow within the structure?

Karin Zojer

And I have to say it was perfectly involuntary. We had just to recognise that we precluded everything. It was not our aim, but you are perfectly right, so a bit lower level of sizing would be the way to go.

Gil Garnier

The good news is we can calculate the diffusion constant of water to the cell wall thanks to your result?

Karin Zojer

This is something, yes absolutely.

Peter de Clerck Papertech Solution Pte Ltd

In industrial practice, we find it extremely difficult to hard size paper to a Cobb value below 18. Do you think that this relates to the water residing in the pores, on the emptying of the pores, and therefore what is retained in the fibre within itself? Is that a limiting factor, and would it relate to your work?

Karin Zojer

That is a very difficult question as I am by no means a paper maker. The hydrophobisation itself, I think, is a very complex process to understand and at least I have not been able to find too many hints how this is going to work in reality. So my understanding is, please contradict me immediately if I have the wrong idea, hydrophobising molecules are molecules whose head group is meant to bind on the fibres somehow and the tail group is responsible for ordering the molecules, so they form, at least to a certain extent, domains with a fair order, and this domain formation itself is a very intricate dynamic process that is occurring on the scale of the fibre surface, possibly strongly dependent on the state of the surface before, and on the available water. I come from microelectronics where they use this to clean surfaces. They do this in conditions in such a way that the docking is happening very efficiently and still the molecules are mobile enough to meet each other on the surface. So, if it has no beneficial effect, at least the surface is cleared of other rubbish.

Peter de Clerck

I was thinking more about the limiting amount of water where we reach a maximum water repellency with a Cobb value that still remained at about 18, no matter how much sizing agent one puts into the paper. Would that relate to the amount of water that would be absorbed by the cellulose fibres themselves? Would that be a limiting factor?

Karin Zojer

To be honest, I am not sure. I like the question because it tells me again there is some interplay between the liquids. You guys are interested in the saturated vapour that is going to be formed around this liquid.

Alexander Bismarck University of Vienna

Just wondering how did you hydrophobise your fibres? You did not quite tell us.

Discussion

Karin Zojer

I did not quite tell you and we did not really hydrophobise the fibres also. This must be very seriously stated. This is machine-made paper, so it came out of the paper mill and had undergone their hydrophobisation procedure. So, it is a paper surface treatment, not a fibre surface treatment. Just the surfaces have been treated like Gil was already mentioning. There are certainly gradients of those molecules if you go into the depth of the paper sheet.

Alexander Bismarck

But then I wonder why the water did not condense in the capillaries of the fibre bridges because there the curvature is high enough for water to condense as well?

Karin Zojer

To be honest, I cannot answer that.